Available online at www.sciencedirect.com
SCIENCE DIRECT®
Carbon 42 (2004) 2025–2032
CARBON
www.elsevier.com/locate/carbon

Important issues in a molecular dynamics simulation for characterising the mechanical properties of carbon nanotubes

K. Mylvaganam, L.C. Zhang

School of Aerospace, Mechanical and Mechatronic Engineering, The University of Sydney, NSW 2006, Australia

Received 22 October 2003; accepted 5 April 2004
Available online 12 May 2004

Abstract

This paper discusses several important issues in a molecular dynamics simulation for analysing carbon nanotubes and their mechanical properties. In particular, the paper addresses the problems in selecting appropriate inter-atomic potentials, number of thermostat atoms, thermostat techniques, time and displacement steps and number of relaxation steps to reach the dynamic equilibrium. Based on these, the structural changes of armchair and zigzag nanotubes and their mechanical properties are investigated. The Young's modulus and Poisson's ratio of the armchair tube are 3.96 and 0.15 TPa, respectively, and those of the zigzag tube are 4.88 and 0.19 TPa, respectively. The best simulation technique identified in this study predicts that the ultimate tensile strain of a carbon nanotube is around 40% before atomic bond breakage.

Keywords: A. Carbon nanotubes; C. Molecular simulation; D. Mechanical properties

1. Introduction

Carbon nanotubes have attracted tremendous attention since their discovery in 1991 [1]. Experimentally they have been observed as single-walled nanotubes (SWNT) [2,3], multi-walled nanotubes (MWNT) [1,4,5], bundles [6,7] and nanoropes [8,9]. They have remarkable electrical and mechanical properties. For example, they have a tensile strength twenty times that of high strength steel alloys and have a current carrying capacity 1000 times that of copper [10]. As such, carbon nanotubes (CNTs) are expected to have a variety of applications, such as in memory chips, sensors, probes, tips and reinforcing phase in composite materials.

With the rapidly growing interest in carbon nanotubes and the difficulties in direct measurements of their properties due to its nanoscale dimension, molecular dynamics simulation has been widely used in characterising the mechanical properties and understanding the mechanisms of deformation. However, such simulations have to be done carefully to represent a behaviour that is believed to be the best representation of reality. First, it is important to select an appropriate interaction potential that effectively describes the deformation of a nanotube correctly to the best of one's knowledge. Secondly, during a loading process, improper treatment of the temperature rise can lead to fictitious results. In molecular dynamics, heat conduction is accomplished via the so-called thermostat atoms and various thermostatting methods. Adiabatic relaxation method, isokinetic thermostatting, Andersen stochastic thermostatting and Nose–Hoover feedback thermostatting were all reported in the literature for temperature conversion [11]. For small systems that are practical for molecular dynamics studies, the adiabatic relaxation method often leads to a fluctuation of the vibrational-relaxation rate. In isokinetic thermostatting, the temperature is maintained in different ways. For example, in the Berendsen thermostat scheme with velocity scaling, the velocities of thermostat atoms are scaled to fix the total kinetic energy. In the Gaussian feedback or Evans–Hoover scheme with force scaling, however, the kinetic energy is monitored and information is fed back into the equations of motion so that the kinetic energy is kept

Tel.: +61-2-9351-7145; fax: +61-2-9351-7060 (K. Mylvaganam); tel.: +61-2-9351-2835; fax: +61-2-9351-7060 (L.C. Zhang).
E-mail addresses: kausala@aeromech.usyd.edu.au (K. Mylvaganam), zhang@aeromech.usyd.edu.au (L.C. Zhang).

0008-6223/$ - see front matter © 2004 Elsevier Ltd. All rights reserved.
doi:10.1016/j.carbon.2004.04.004

constant to dissipate heat by controlling the thermostatting force. The velocity scaling has been used in general because it is a simpler scheme to implement. For small time steps, the Gaussian isokinetic method and velocity scaling method are identical [11]. However, a very small time step will give an unusually high elongation speed. On the other hand, a small displacement step with a small time step will be computationally expensive. The flaw in the isokinetic-thermostatting method is that it is impossible to separate the effects of thermostatting on rate processes. The other two schemes also have this limitation to a certain extent. Thirdly, a system has to be relaxed initially as well as during the simulation so that the velocities of the Newtonian and thermostat atoms reach equilibrium at the specified temperature of simulation; thus appropriate time step and displacement step have to be selected to get a reasonable elongation speed.

It is unfortunate that no comparison or clarification is available in the literature as to the key issues aforementioned for a molecular dynamics simulation of carbon nanotubes. For example, researchers have used either the Tersoff–Brenner potential or the tight binding potential in their molecular dynamics calculations on nanotubes. Those who used the former claimed that the potential was selected because it could avoid the overbinding of radicals. Sinnot and co-workers [12,13] used the first few rows of atoms on both ends of a CNT as boundary atoms and the next few rows as thermostat atoms applying the Langevin heat baths. Zhou and Shi [14] used the first two rows of atoms on both ends of a CNT as boundary atoms but treated all the other atoms as thermostat atoms. No information is available on the method of temperature conversion. Moreover, various time steps, ranging from 0.15 to 15 fs, have been used in the simulation of carbon nanotubes. A natural question is therefore: Which simulation scheme will be more appropriate and effective?

This study aims to come up with the necessary details such as the potential, number of thermostat atoms, thermostat method, time step, displacement step and the number of relaxation steps that are key to the simulation of carbon nanotubes.

2. Simulation model

The inter-atomic forces were described by the Tersoff (T) potential [15,16] and the empirical bond order potential formulated by Brenner based on Tersoff potential and known as Tersoff–Brenner (TB) potential [17,18]. The simulations were carried out at 300 K with Berendsen (B) and Evans–Hoover (EH) thermostats and a time step of 0.5 fs. Open single-walled armchair nanotube (10,10) with 100 repeat units along the axial direction and zigzag nanotube (17,0) with 58 repeat units along the axial direction, both having a length of about 245 Å, were examined with different schemes as detailed below:

2.1. Scheme 1 (S1)

In this scheme, the first two layers of atoms on both ends of a CNT were held rigid. The next four layers were taken as thermostat atoms and the remaining were treated as Newtonian atoms. First, the tubes were annealed at the simulation temperature for 5000 time steps. Then the rigid atoms on both ends were pulled along the axial direction at an increment of 0.05 Å unless otherwise stated in the discussion. Each displacement step was followed by 1000 relaxation steps in order to dissipate the effect of preceding displacement step over the entire length of the tube.

2.2. Scheme 2 (S2)

In this scheme, all atoms except the boundary ones rigidly held were treated as thermostat atoms as described in Ref. [14]. In this case, each displacement step was followed by 50 relaxation steps (in Section 3.4, different number of relaxation steps were used to examine this).

3. Results and discussion

3.1. Stress–strain relationship

The axial tensile stress in a carbon nanotube as a function of strain was calculated by dividing the axial force by the cross-sectional ring area of the nanotube. The equivalent wall thickness of a SWNT is taken as 0.617 Å [19] which gives the area as 2.582×10^{-19} m^2.

Fig. 1 shows the stress–strain relationships of the armchair (10,10) and zigzag (17,0) CNTs using the T and TB potentials with Berendsen and Evans–Hoover thermostats. It is clear that all the stress–strain curves have four distinct stages. Stage 1 is the initial linear region, to a strain of about 0.06, followed by stage 2 where the stress–strain curve conforms to plateau. The stress increases rapidly and reaches its peak in stage 3, and in most cases, except TB(E-H) and TB(B3), abruptly drop to zero or close to zero in stage 4. The Young's moduli of the CNTs were evaluated from the linear region (stage 1), which gave a value of 3.96 TPa for the armchair nanotube and 4.88 TPa for the zigzag nanotube, which shows that the bond orientation in zigzag tube increases the stiffness. As pointed out by Vodenitcharova and Zhang [19], the value of the Young's modulus of a nanotube depends on the effective wall thickness of the CNT. Here we use the equivalent thickness of 0.617

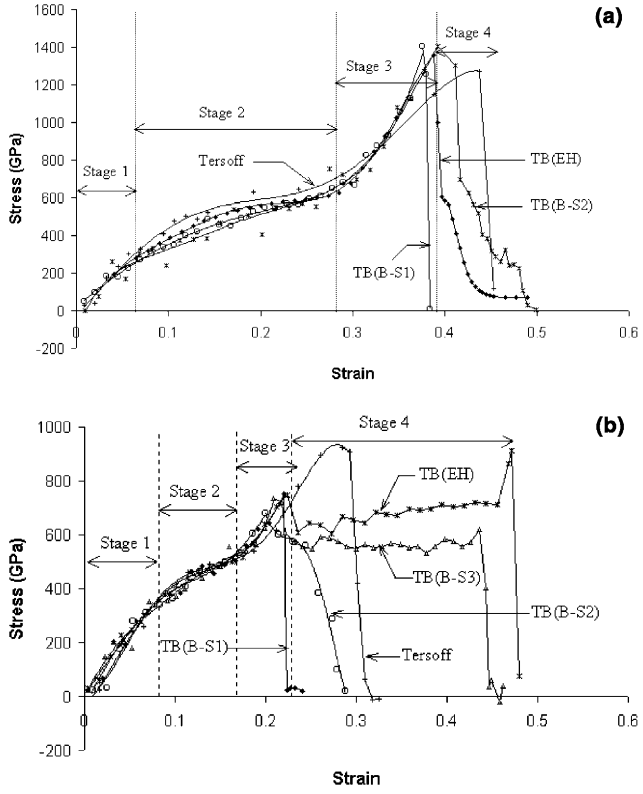

Fig. 1. The stress–strain curves of (a) a (10,10) armchair SWNT and (b) a (17,0) zigzag SWNT using Tersoff and Tersoff–Brenner potentials. In the figure, TB(B-S1) is the calculation with Berendsen thermostat and Scheme 1 simulation details; TB(B-S2) is the calculation with Berendsen thermostat and Scheme 2 simulation details and TB(B-S3) is the calculation as in TB(B-S2) but with a smaller displacement step of 0.008 Å. TB(EH) is the calculation with Evans–Hoover thermostat.

Å as mentioned at the beginning of this section. [1] The Poisson's ratios, $(\Delta r/r)/(\Delta l/l)$, were found to be 0.15 for the armchair CNT and 0.19 for the zigzag CNT, where Δr and Δl are the changes in tube radius, r, and tube length, l, respectively.

3.2. Inter-atomic potential

At the initial stage of loading, all the stress–strain curves overlap and are almost linear. Thereafter, the Tersoff potential curve lies slightly above the Tersoff–Brenner potential curves but they have the same trend up to a strain of 0.34 and 0.2 for the armchair and zigzag CNTs, respectively. The armchair CNT has the maximum stress of about 1357 GPa around a strain of 0.4 and the zigzag CNT has the maximum stress of 754 GPa around a strain of 0.22. After this, a large cross-sectional necking happens. If the CNTs are unloaded just prior to the maximum stress, the stress–strain curve at unloading overlaps with the loading one, showing that the CNT deformation up to this stage is completely elastic.

At various stages of the loading process, the structural changes can be examined by unrolling the CNTs. Figs. 2 and 3 give the unrolled view of a portion of the armchair and zigzag CNTs at stages 1–3 when using the TB potential. It is shown that during loading both the bond angles and bond lengths change. In the zigzag CNT, the bonds are stretched along the loading axis, due to the way they orient.

For an armchair CNT, Fig. 4(a) and (b) compare the variation of these geometrical parameters. With the TB potential, the change in bond angles is more but with the Tersoff potential the change in bond lengths is more. At about maximum loading, some of the stretched bonds are broken and the Tersoff potential curve starts to deviate from the TB curve. This seems to indicate that when bonds are broken, radicals will form and hence the over-binding effect that was not considered in the development of Tersoff potential would become important. The TB potential results showed the necking of the tube followed by the formation of a one-atom chain, as shown in Figs. 5 and 6. The use of the Tersoff potential, however, did not bring about any necking or formation of a one-atom chain, and the tube broke suddenly after reaching the maximum stress.

The above comparison and discussion show that the TB potential describes the whole process reasonably well. However, the Tersoff and TB potential curves overlap at the initial stages, suggesting that the Tersoff potential can be used for the calculation of the mechanical properties of a carbon nanotube such as the Young's modulus and Poisson's ratio.

3.3. Number of thermostat atoms

It is necessary to clarify the issue because in the literature the number of thermostat atoms were selected and used without a rational reason. Our comparison was done with the Tersoff–Brenner potential using the Berendsen thermostat.

Scheme 1 showed little fluctuation in temperature up to the third stage. In stage 4, the tube begins to fall into pieces, resulting in a sudden and rapid increase in temperature caused by energy released from atomic bonds that are being broken simultaneously. Moreover, with such an arrangement of thermostat atoms, no significant necking takes place.

With Scheme 2 a remarkable necking occurs in stage 4. The armchair tube started necking at a strain of 0.39 and the zigzag tube started its necking at a strain of 0.22. The temperature increase in this stage was only 20–30 K.

[1] As clarified in Ref. [19], it is incorrect to use graphite interplanar spacing of 3.44 Å as the effective wall thickness of a SWNT, as many researchers did in experimental and theoretical characterisation of Young's modulus. In the present calculation, if this value (i.e. 3.44 Å) is used, then the Young's moduli of armchair and zigzag nanotubes will become 0.7 and 0.87 TPa, respectively.

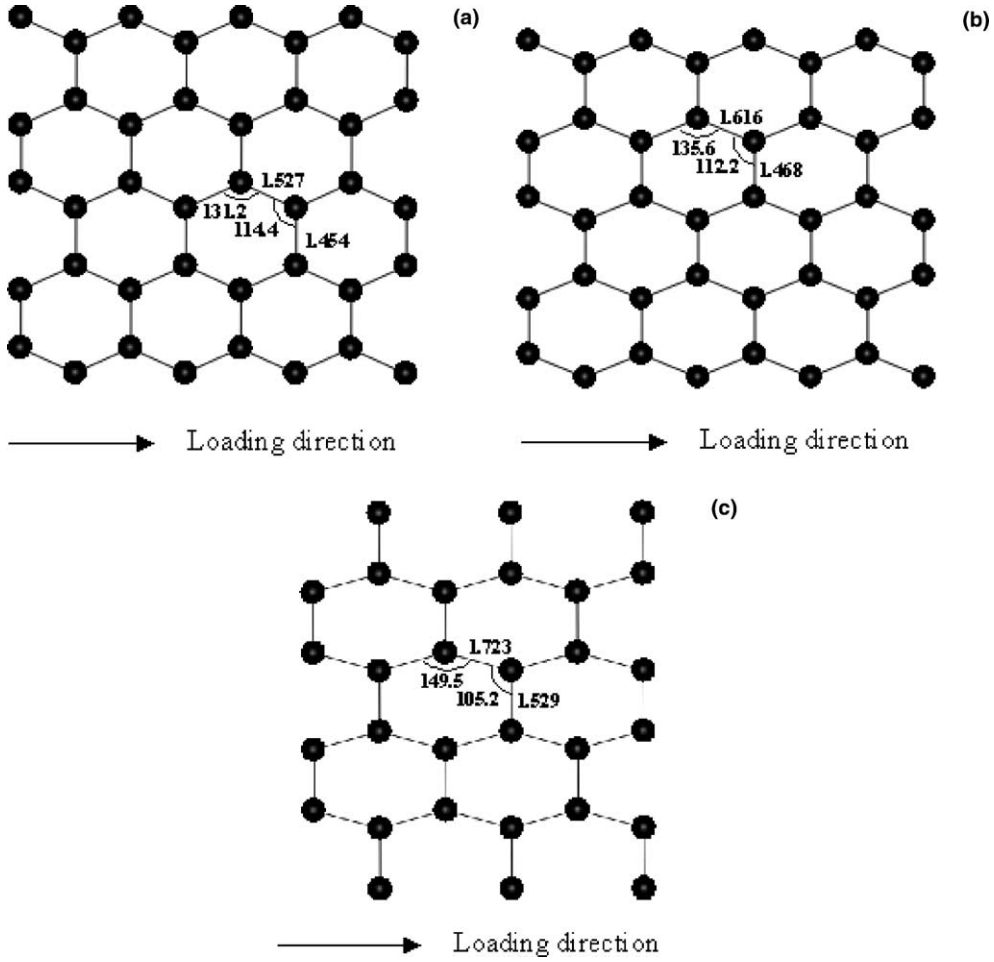

Fig. 2. Structural changes of an armchair tube (10,10) in (a) stage 1, (b) stage 2 and (c) stage 3; the bond lengths are in angstroms and the bond angles are in degrees.

On further application of the tensile force, a one-atom chain formed as shown in Figs. 5 and 6, and it grew with the applied force before the tube broke as reported in the literature [14,20]. Within the chain, the strain was constant with a C–C distance of 1.7 Å. In other words, on further pulling the C–C distance in the atomic chain did not change but more and more C atoms joined the chain. This is known as the carbon chain unravelling and it was observed in an experiment when a capped nanotube was opened by the force of an electric field [21]. However, analysis of the current molecular dynamics results showed that the electronic structure of this chain is neither close to the cumelenic form nor to the bond alternate polyyne as suggested in Ref. [21]. It is believed to be a pure unravelling process that originates from a place where a bond is broken. Although in chemical terms the valency of carbon is not satisfied, it may be possible to have such a chain under stress. Once the growing chain got detached from the tube, the C–C distance decreased to 1.33 Å that is equivalent to C–C double bond as in the cumelenic form. During necking, some bonds were broken and some new bonds were formed to facilitate the closure of the ends at the breakage. As a result, the temperature did not go up suddenly. The slight increase in temperature may be attributed to the activation energy of the unravelling process.

It should be noted that the loading rate in molecular dynamics calculations is much higher compared to that in experiments. As such, not much heat will be generated in an experiment. In the simulations, because of the computational cost and numerical accuracy, the loading rate cannot be as low as in the experiment. Hence one has to find an effective way to conduct the heat that is produced as a result of the higher loading rate. This could be achieved either by relaxing the atoms for a long time between each step of pulling, which is computationally expensive, or by treating all the atoms as thermostat atoms as in Scheme 2. Scheme 1 is not reliable in this sense because the Newtonian atoms are not fully surrounded by the thermostat atoms; i.e. they are exposed to the environment. As such, the heat conduction in the simulation cannot reflect the true deformation process of a nanotube under experimental conditions.

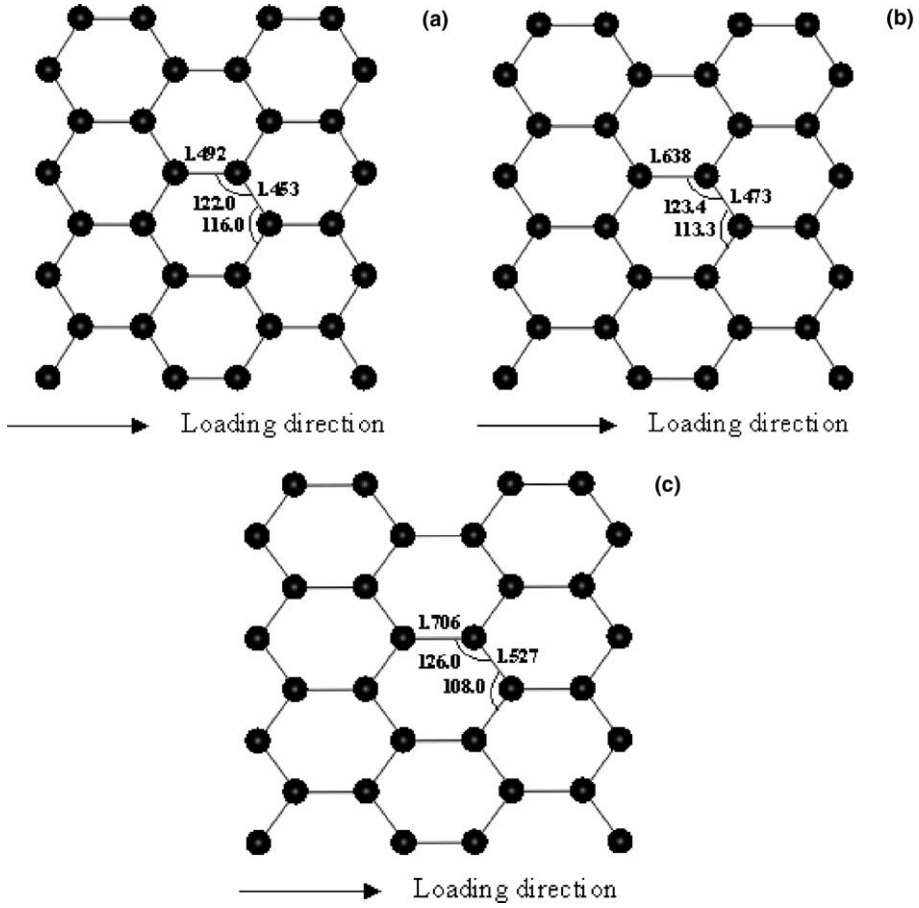

Fig. 3. Structural changes of a zigzag tube (17,0) in (a) stage 1, (b) stage 2 and (c) stage 3; the bond lengths are in angstroms and the bond angles are in degrees.

This means that Scheme 2 is the right one to use in molecular dynamics simulation of carbon nanotubes.

3.4. Dependency on thermostat techniques

Heat conversion is a central component in a correct molecular dynamics simulation [22,23]. An inappropriate conversion technique results in incorrect atomic motion and deformation. To examine the effect of thermostat techniques, we use TB potential, as it gives more reasonable results for carbon nanotubes. For the armchair tube, both Berendsen and Evans–Hoover thermostats gave similar results until the maximum stress. After this point, with the Berendsen thermostat the stress dropped down to zero, the temperature went up and the tube broke into pieces without the formation of an atomic chain; with the Evans–Hoover thermostat and the Berendsen thermostat with Scheme 2, the stress dropped down to a value close to zero, and the tube necked, formed an atomic chain and then broke into two pieces with closed ends.

With the Evans–Hoover thermostatting technique, the zigzag tube showed an entirely different behaviour from the armchair tube once the maximum stress was reached. The zigzag tube started to neck at both ends at a strain of 0.23 as with Berendsen technique, but on further tension the necking propagated as shown in Fig. 7(a) until the whole tube became narrow at a strain of 0.47. In this period the stress was almost constant. This could be because, in the zigzag tube, both types of bonds can get stretched as shown in Fig. 7(b) and hence the necking and its propagation as shown in Fig. 7(a) is possible; whereas in the armchair tube, the C–C bonds that are normal to the direction of pulling cannot get stretched; hence the stretched bonds will break once it reaches the maximum stress. On further application of the tensile force, again, the tube necked at both ends, formed a one-atom chain and broke within a short period. It is interesting to note that the ultimate failure of the tube happens around a strain of 0.475, which is close to that of an armchair tube.

The Evans–Hoover technique can be understood more easily if the discussion in Section 1 is recalled. In this technique, the force scaling is done on all atoms irrespective of the number of thermostat atoms used in the calculation and the kinetic energy is kept constant.

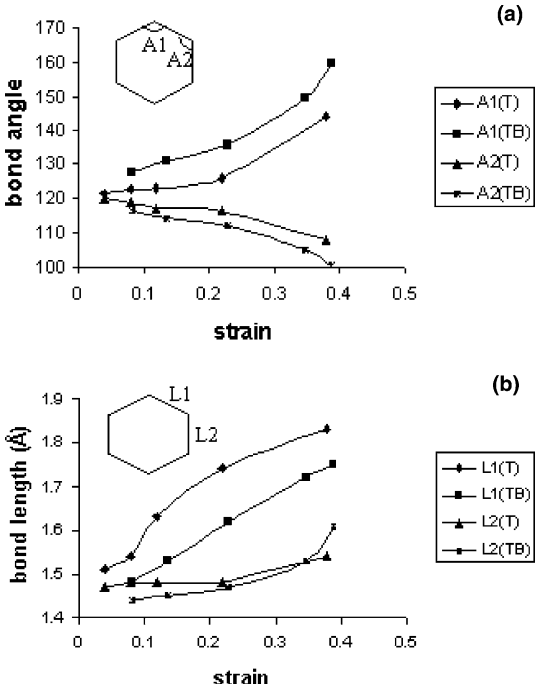

Fig. 4. Comparison of the change in (a) bond angles (A1 and A2) and (b) bond lengths (L1 and L2) of an armchair CNT with the Tersoff and Tersoff–Brenner potentials.

Thus the heat conduction problem is avoided and a very smooth stress–strain curve can be obtained. However, with this technique one has to work with small time steps. This means that in order to have a reasonable loading rate, the displacement step must be small, which would significantly increase the overall computational time. Hence, if the Berendsen technique with Scheme 2 is used, one can minimise the heat conduction problem and improve the computational efficiency.

3.5. Integral time step, displacement step and number of relaxation steps

In molecular dynamics simulation, the time step has to be selected to reduce the round-off error and truncation error. A suitable time step should be less than 10% of the vibration period of an atom and accordingly, for diamond, a time step of 0.5–0.8 fs provides good results. Hence in our calculations, we have used a time step of 0.5 fs.

Displacement step is usually chosen according to the time step used. For the armchair tube, variation in the displacement step did not show any significant difference in the stress–strain relationship. However, for the zigzag tube, the Berendsen technique with Scheme 2 and a displacement step of 0.05 Å showed failure at a strain of 0.23. When the displacement step was reduced to 0.008 Å, the tube necked and the necking propagated over the entire length of the tube and then formed one atom chain at the strain of 0.44, which is similar to the result from the Evans–Hoover thermostatting technique. In other words, a little lower elongation speed showed a more reasonable results (refer to the explanation given in Section 3.3). Moreover, on unloading from a point within a strain of 0.23–0.44, the results showed that the deformation was still elastic although the unloading curve took a different path until a strain of 0.182. This is because on unloading the bond lengths and bond angles do not change in the same way as in loading.

Initially the tube is relaxed to its dynamically equilibrium status at the specified simulation temperature. We found that to reach this equilibrium about 4000 relaxation steps are required. As a result, in all of our calculations the initial relaxation was done for 5000 steps. After the initial relaxation, tensile loading was

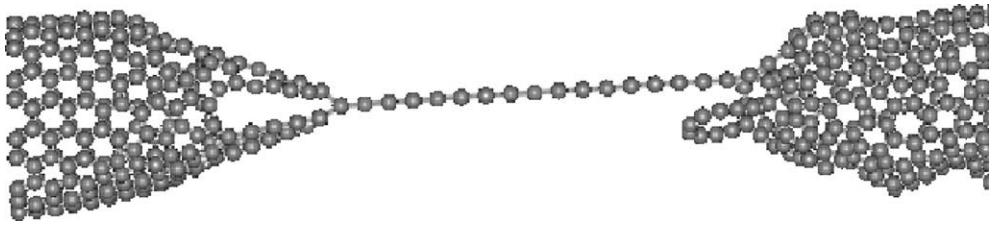

Fig. 5. Atomic chain of an armchair tube when using Berendsen thermostat.

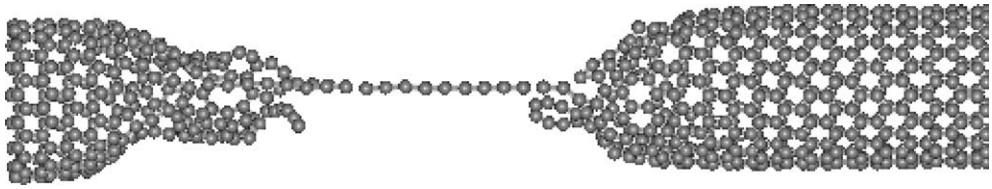

Fig. 6. Atomic chain of a zigzag tube when using Berendsen thermostat.

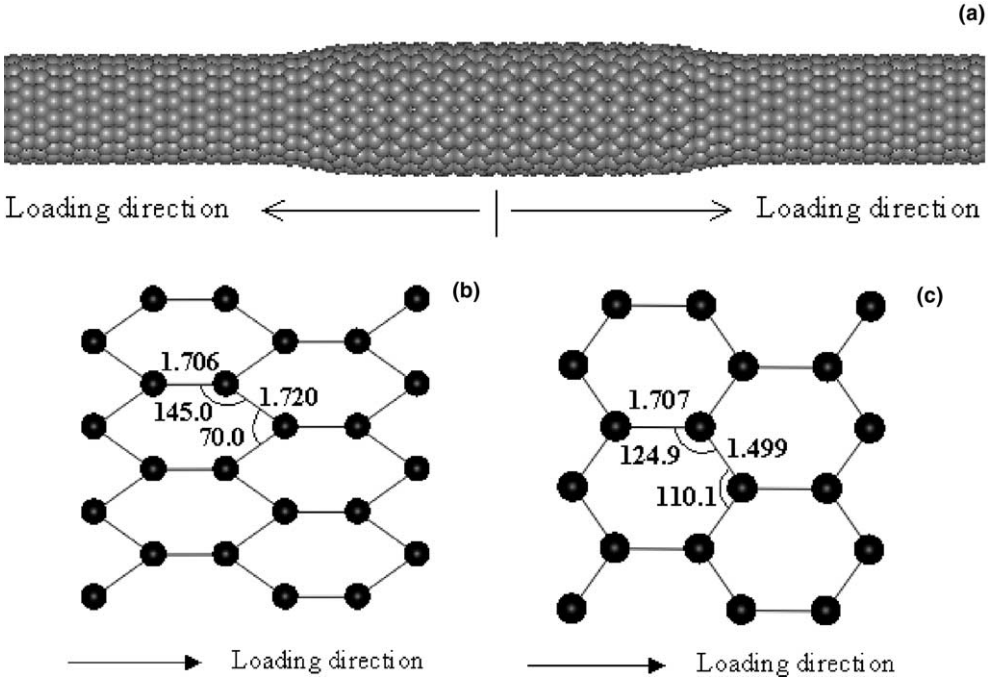

Fig. 7. The deformation of a zigzag carbon nanotube. (a) Necking that propagates along the tube, (b) the structure when unrolling the tube at the necking part of (a), (c) the structure when unrolling the central part of (a).

applied via small displacement steps. The effect of the displacement was dissipated over the entire length of the tube and subsequently a dynamic equilibrium was achieved by relaxing the system after each displacement. The required number of relaxation steps varies with the number of thermostat atoms used. Scheme 1, as explained in Section 3.2, required nearly 1000 relaxation steps to reach dynamic equilibrium. Even though, necking and one-atom-chain formation was not observed. On the other hand, Scheme 2 with 50 relaxation steps showed necking and one-atom-chain formation for both armchair and zigzag nanotubes as observed by other researchers.

These results clearly show that even with 20 times the relaxation steps used in Scheme 2, Scheme 1 fails to show the necking once the maximum stress is reached. For the zigzag tube a smaller displacement step of 0.008 Å is required, in order to have the ultimate failure of the tube around a strain of 0.44.

4. Conclusions

(i) The simulation using Tersoff–Brenner potential and Berendsen thermostat with all atoms as thermostat atoms (except the rigid ones) and 50 relaxation steps after each displacement of 0.008 Å is a more reasonable and cost effective method.
(ii) Following the reasonable approach, it is quantified that the Young's modulus and Poisson's ratio of (i) the armchair tube are 3.96 and 0.15 TPa, respectively and (ii) the zigzag tube are 4.88 and 0.19 TPa, respectively. The armchair tube can undergo a higher tensile stress compared to the zigzag tube. Under tension, both armchair and zigzag nanotubes exhibit carbon chain unravelling and one-atom chain at a strain of around 0.4.

Acknowledgements

The authors would like to thank the Australian Research Council for the continuous financial support. Part of this work was done with the support from the Australian partnership for advanced computing. L.G. Zhou and S.Q. Shi answered promptly our queries on their published work.

References

[1] Iijima S. Helical microtubules of graphitic carbon. Nature 1991; 354:56–8.
[2] Iijima S, Ichlhashi T. Single-shell carbon nanotubes of 1 nm diameter. Nature 1993;363:603–5.
[3] Bethune DS, Klang CH, Devries MS, Gorman G, Savoy R, Vazquez J, et al. Cobalt-catalyzed growth of carbon nanotubes with single-atomic-layer walls. Nature 1993;363:605–7.
[4] Ebbesen TW, Ajayan PM. Large-scale synthesis of carbon nanotubes. Nature 1992;358:220–2.

[5] Zhao X, Ohkohchi M, Wang M, Iijima S, Ichihashi T, Ando Y. Preparation of high-grade carbon nanotubes by hydrogen arc discharge. Carbon 1997;35:775–81.
[6] Qiu J, Li Y, Wang Y, Wang T, Zhao Z, Zhou Y, et al. High-purity single-wall carbon nanotubes synthesized from coal by arc discharge. Carbon 2003;41:2170–3.
[7] Cheng HM, Li F, Su G, Pan HY, He LL, Sun X, et al. Large-scale and low-cost synthesis of single-walled carbon nanotubes by the catalytic pyrolysis of hydrocarbons. Appl Phys Lett 1998;72:3282–4.
[8] Thess A, Lee R, Nikalaev P, Dai H, Petit P, Robert J, et al. Crystalline ropes of metallic carbon nanotubes. Science 1996;273:483–7.
[9] Cheng HM, Li F, Sun X, Brown SDM, Pimenta MA, Marucci A, et al. Bulk morphology and diameter distribution of single-walled carbon nanotubes synthesized by catalytic decomposition of hydrocarbons. Chem Phys Lett 1998;289:602–10.
[10] Collins PG, Avouris P. Nanotubes for electronics. Scientific American 2000;283:62–9.
[11] Holian BL. Simulations of vibrational relaxation in dense molecular fluids. In: Ciccotti G, Hoover WG, editors. Molecular-dynamics simulation of statistical–mechanical systems. Elsevier Science Publishers B.V.; 1986. p. 241–59.
[12] Garg A, Sinnott SB. Molecular dynamics of carbon nanotube proximal probe tip-surface contacts. Phys Rev B 1999;60:13786–91.
[13] Ni B, Sinnott SB, Mikulski PT, Harrison JA. Compression of carbon nanotubes filled with C_{60}, CH_4 or Ne: predictions from molecular dynamics simulations. Phys Rev Lett 2002;88:205505.
[14] Zhou LG, Shi SQ. Molecular dynamic simulations on tensile mechanical properties of single-walled carbon nanotubes with and without hydrogen storage. Compos Mater Sci 2002;23:166–74.
[15] Tersoff J. New empirical model for the structural properties of silicon. Phys Rev Lett 1986;56:632–5.
[16] Tersoff J. Modeling solid-state chemistry: Interatomic potentials for multicomponent systems. Phys Rev B 1989;39:5566–8.
[17] Brenner DW. Empirical potential for hydrocarbons for use in simulating the chemical vapor deposition of diamond films. Phys Rev B 1990;42:9458–71.
[18] Brenner DW, Shenderova OA, Harrison J, Stuart SJ, Ni B, Sinnott SB. A second-generation reactive empirical bond order (rebo) potential energy expression for hydrocarbons. J Phys: Condensed Matter 2002;14:783–802.
[19] Vodenitcharova T, Zhang LC. Effective wall thickness of a single-walled carbon nanotube. Phys Rev B 2003;68:165401–4.
[20] Yakobson BI, Campbell MP, Brabec CJ, Bernholc J. High strain rate fracture and c-chain unraveling in carbon nanotubes. Compos Mater Sci 1997;8:341–8.
[21] Rinzler AG, Hafner JH, Nikolaev P, Lou L, Kim SG, Tomanek D, et al. Unravelling nanotubes: field emission from an atomic wire. Science 1995;269:1550–3.
[22] Zhang LC, Tanaka H. On the mechanics and physics in the nano-indentation of silicon monocrystals. JSME Int J Series A 1999;42:546–59.
[23] Cheong WCD, Zhang LC, Tanaka H. Some essentials of simulating nano-surfacing processes using the molecular dynamics method. Key Eng Mater 2001;196:31–42.